

# Laser Measurements of Solid-Particle Rebound Parameters Impacting on 2024 Aluminum and 6A1-4V Titanium Alloys

W. Tabakoff,\* M.F. Malak,† and A. Hamed‡  
University of Cincinnati, Cincinnati, Ohio

This paper describes an experimental method used to find the particle restitution coefficients. The equations that govern the motion of solid particles suspended by a compressible gas flow through a turbomachine depend on the restitution coefficients. Analysis of the data obtained by the laser Doppler velocimeter system of the collision phenomenon gives the restitution ratios as a function of the incidence angle. From these ratios, the particle velocity components after collision are computed and used as the initial conditions to the solution of the governing equations of motion for the trajectory of the particles. The erosion of metals impacted by small dust particles can be calculated by knowing the restitution coefficients. The alloys used in this investigation are 2024 aluminum and 6A1-4V titanium.

## Introduction

AIRCRAFT engines operating in areas where the atmosphere is polluted by small solid particles and industrial gas turbines burning coal as fuel are examples of machines operating under particulate two-phase flow conditions. The presence of solid particles in the working media leads to a performance deterioration of these engines, both structurally and aerodynamically.

Under two-phase flow conditions, the gas and particles experience different degrees of turning as they flow through the blade channels. This is mainly due to the differences in their inertia. The major interacting force between the gas and particles is the viscous drag. The degree of turning and acceleration or deceleration achieved by the particles depends on the ratio of the viscous forces to the inertial forces experienced by the particles. This results in a concentration gradient across the blade channel and causes a change in the properties of gas and particles. The net result is a change in the blade surface pressure distribution, which alters the engine performance during the period of particle ingestion.

If the particles are of erosive nature, the problem becomes more complicated. The impact of particles on the blade surfaces can cause severe erosion damage, leading to structural failure of the blades. This damage is manifested by pitting and cutting of the blade leading and trailing edges and a general increase in the blade surface roughness. The overall effect of these phenomena, from the aerodynamic viewpoint, is an increase in total pressure loss across the blade row.

The use of pulverized coal as fuel in many powerplants and industrial establishments is inevitable, both currently and in the future. The major problem confronting earlier developers of coal-burning turbines is the serious erosion of turbine blades and other metal parts by the suspension of fly ash in hot combustion gases. It is possible to remove approximately 85% by weight of the ash in these gases using cyclones. However, small particles of 1–15  $\mu\text{m}$  still pass through the

cyclones and enter the turbine. Typical ash concentrations for such a turbine are about 0.000275 mg/cm.<sup>3</sup> The damage is caused principally by erosion of the leading and trailing edges of the stator and rotor blades. A thorough knowledge of the various parameters influencing the extent of erosion damage is required to improve the life and the aerodynamic performance of turbomachinery operating in an ambient of particulate flow. This paper presents an experimental method of determining the particle restitution coefficients used for trajectory calculations in turbomachinery and in the new derived equations to calculate the material erosion.

## Experimental Setup

The experimental setup is shown schematically in Fig. 1. It consists of erosion wind tunnel and solid particle feeder.

### Erosion Wind Tunnel

Existing erosion wind tunnel was used in this investigation.<sup>1</sup> The major advantage of this tunnel is its ability to control the primary variables of fluid velocity, particle velocity, particle flow rate, and particle sizes in a representative aerodynamic environment. Provisions are made in the tester design to allow variation between the angle of attack of the abrasive particle and the surface of the test specimen.

Figure 1 is a schematic description of the apparatus to fulfill these objectives. The equipment functions as follows. A measured amount of dry fly ash is placed into the particle feeder A. The particles are fed into secondary air source and carried up to the particle injector C, where they mix with the main air supply B. The particles are then accelerated by the high-velocity air in a constant area duct D and impact the specimen in test section E. The test dust is then separated from the air by a cyclone separator G and collected in the container H. The test air is further filtered through a commercial 5  $\mu\text{m}$  filter F.

The test section is designed such that the particle-laden air is channeled over the specimen and the aerodynamics of the fluid surrounding the blade sample is preserved. This section contains several interchangeable inserts such that the fluid profile can be determined using conventional instrumentation and the particle trajectories can be recorded using high-speed photographic or laser methods.

### Particle Feeder

The particles from the feeder A (Fig. 1) are carried up to the particle injector. The feeder is designed as a vessel to operate at high air pressures. However, this pressure is

Presented as Paper 85-1570 at the AIAA 18th Fluid Dynamics, Plasma Dynamics and Lasers Conference, Cincinnati, OH, July 16-18, 1985; received Nov. 4, 1985; revision submitted Aug. 7, 1986. Copyright © American Institute of Aeronautics and Astronautics, Inc., 1986. All rights reserved.

\*Professor, Department of Aerospace Engineering and Engineering Mechanics. Fellow AIAA.

†Graduate Research Assistant, Department of Aerospace Engineering and Engineering Mechanics.

‡Professor, Department of Aerospace Engineering and Engineering Mechanics. Associate Fellow AIAA.

equalized above and below the plunger by a bypass line. This allows the system to be calibrated under gravity feed conditions. Further, an electric eye records the plunger rpm such that the operating conditions are maintained. The metering orifice is designed to be replaceable. In this manner, a larger (or smaller) orifice may be used, along with corresponding rod diameter, to allow versatility of the feeder. In this investigation, the airflow was seeded with fly ash with size distribution as shown in Table 1. The chemical composition of the fly ash is given by Kotwal and Tabakoff<sup>2</sup> (Si 50%, Al 22%, Fe 20%, S 1.2%, with the remainder being Mg, NA, Ca, C, etc.).

#### Laser and Optics (LDV System)

The optical elements of the two-component laser Doppler anemometer were arranged in the backward scatter mode to measure two simultaneous velocity components of a single particle using two counter processors. A two-color 5 W argon-ion Spectra physics, model 164-09 was used as laser source. The laser beams are brought into one common measuring volume using a transmitting lens of 250 mm focal length. The crossing angle for the incident 1.5 mm diam beams was 11.05 deg.

The laser Doppler velocity (LDV) and the measuring volume characteristics are shown in Table 2.

#### Data Acquisition System

Two signal processors TSI model 1990 and on-line Minc 11/23 are used to acquire synchronized data for the simultaneous measurements of the two velocity components. The minimum time for a particle to cross the measuring volume was evaluated to be 1.4  $\mu$ s. Accordingly, the synchronization condition was set to 1  $\mu$ s, which is the time out between the two data ready pulses received from both signal processors. A time out of 5  $\mu$ s, after each valid synchronized data point is tagged in the computer, allows the particle to clear the measuring volume. The data acquisition program thus insures that the sampling data are not obtained more than once from the same particle.

#### Development of Particle Rebound Correlations

The erosion of metals impacted by small dust particles, as well as the rebound dynamics of these particles, can be described only in a statistical sense. This becomes obvious when one examines the number of geometric situations that might occur at impact. After a given incubation period, the target material will become pitted with craters and, in fact, after a slightly longer period, a regular ripple pattern may form on the eroded surface. Thus, the local impact angle between the small particle and the eroded surface may deviate considerably from the geometric average. Further, the particles themselves are irregularly crystalline in shape with several sharp corners. As the particle approaches the specimen, the orientation of the particle is, for the most part, random. Thus, some particles will impact on a flat surface and do very little work on the target material. Others will impact with a corner oriented in a manner where it will remove material in a method similar to that of a cutting tool.

The restitution coefficient or restitution ratio is a measure of the kinetic energy exchange between two objects upon impact. Since erosion is a function of the energy exchange between the erodent particle and the material impacted, the restitution ratio will give a good indication of the behavior of the

particle/material interaction. In this investigation, an erosive impact occurs when the contaminant particle is much harder than the target material. This investigation was limited to ductile target materials, upon which the particle will create local stresses high enough to cause plastic flow in the target material.

Grant and Tabakoff<sup>3</sup> were the first to investigate thoroughly the rebound characteristics of high-speed eroding particles. Their study was carried out on annealed 2024 aluminum alloy. The data were described using histograms to illustrate its statistical distribution. It was concluded that the restitution ratio  $V_2/V_1$ , which is directly related to the kinetic energy lost during impact, does not give sufficient information with regard to erosion. With this in mind, the restitution ratio was broken down into a normal velocity restitution ratio  $V_{N2}/V_{N1}$  (the normal component of the particle velocity after impact/the normal component of the particle velocity before impact), as shown in Fig. 2, and a tangential velocity restitution ratio  $V_{T2}/V_{T1}$  (the tangential component of the particle velocity after impact/the tangential component of the particle velocity before impact). It was found that the normal velocity restitution ratio does not significantly contribute to ductile erosion. Most probably, the kinetic energy is dissipated by

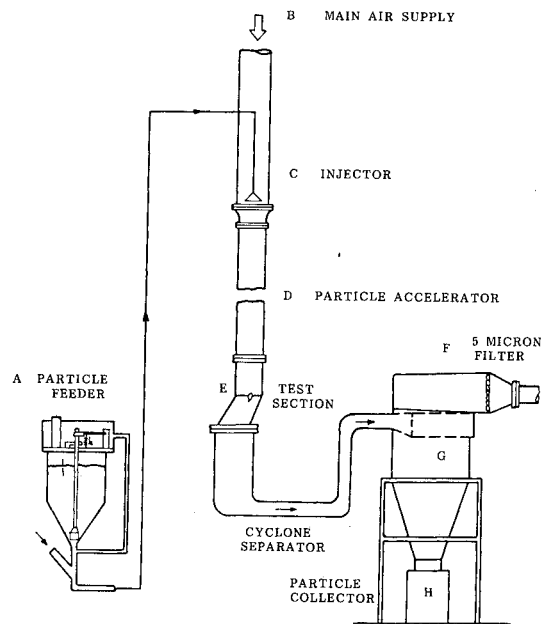


Fig. 1 Erosion research facility.

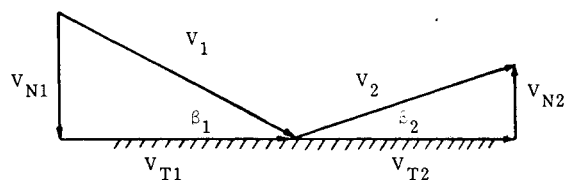


Fig. 2 Velocity and angle notations.

Table 1 Fly ash size distribution

Size, $\mu$ m	Percent
Under 5	62
5-10	17
10-20	20
Over 20	1

Table 2 LDV characteristics

Color	Blue	Green
Wavelength, $\mu$ m	0.448	0.5145
Fringe spacing, $\mu$ m	2.534	2.672
Diameter of measuring volume at $1/e^{-2}$ intensity location, mm	0.1045	0.1097
Length of measuring volume at $1/e^{-2}$ intensity location, mm	1.08	1.134
No. of stationary fringes	41	41

plastic deformation of the target material without significant material removal.

### Measurement Technique

The LDV system was used to measure the impact and rebound velocities and angles on 2024 aluminum, and 6A1-4V titanium samples for different incidence angles. The impinging particle velocities were measured at four points above the sample as shown in Fig. 3.

At point 1, the results obtained include the velocities of the smaller fly ash particles (less than  $2 \mu\text{m}$ ) that follow the airflow streamlines without hitting the specimen surface. Therefore, the velocity at point 2 was selected to represent the impingement velocity for all impacting angles. Measurements for five incidence angles  $\beta_1$  were performed and a summary of the normalized average and standard deviation of the impingement velocities are shown in Table 3. The velocities are normalized with respect to the particle velocity at the center of the test section, which was  $98 \text{ m/s}$  ( $320 \text{ ft/s}$ ). The standard deviation is large due to the irregular shapes of the fly ash particles and the size variation (standard deviation) causes the particles to randomly deviate from the airflow path.

The rebounding velocities were measured at four points located on a line  $0.3 \text{ mm}$  above and parallel to the specimen

surface, as shown in Fig. 4 for all impacting angles. It was found that the variation of the rebounding velocities at these four points were within the standard deviation.

The average rebounding velocities were measured and normalized with respect to the corresponding impact velocities listed in Table 3 for the different impacting angles. The results are shown in Tables 4 and 5.

The ratio of the particle velocity after and before impact  $V_2/V_1$  is plotted against the angle of attack  $\beta_1$  in Fig. 5. Since the statistical distributions are of importance, the shape of these distributions are cross plotted in the figure. The parameter  $V_2/V_1$  is directly related to the kinetic energy lost during impact. The spread in these data indicates the variable condition of the surfaces and the orientation of the particle at impact. It is evident from this figure that  $V_2/V_1$  decreases as the impact angle  $\beta_1$  increases from 0 to  $75 \text{ deg}$ .

The directional coefficient  $\beta_2/\beta_1$  is plotted in Fig. 6 vs the impact angle  $\beta_1$ . Again, these data are plotted with their statistical distributions. The minimum directional coefficients have been found to be at  $\beta_1 = 38 \text{ deg}$ .

Figures 7–10 show the influence of impact angles on erosive particle velocity restitution ratios for different target materials.

The solid lines in Figs. 5–10 represent a least squares polynomial curve fit of the mean value of the restitution parameters. For the 2024 aluminum, these restitution parameters may be expressed by the following equations:

$$e_V = V_2/V_1 = 1.02027 - 0.91773\beta_1 + 0.39453\beta_1^2 + 0.25147\beta_1^3 - 0.21932\beta_1^4 \quad (1)$$

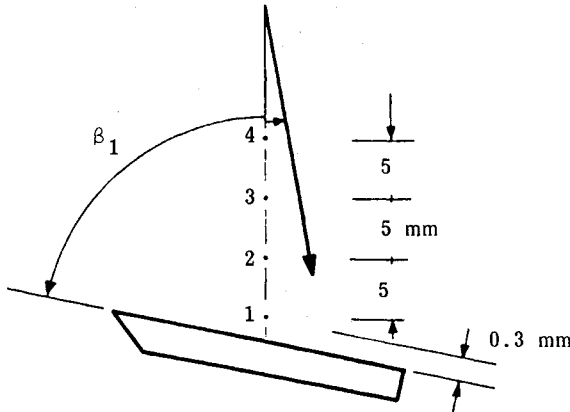


Fig. 3 Impingement measurement locations.

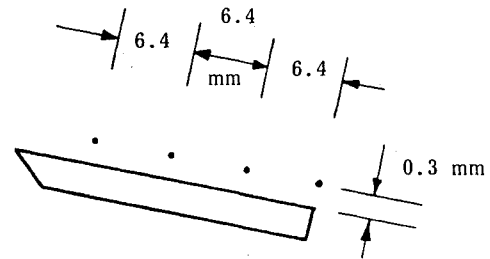


Fig. 4 Rebounding measurement locations.

Table 3 Normalized average impingement velocities at different impact angles

Incidence angle $\beta_1$ , deg	Normalized incidence velocity					
	Tangential		Normal		Total	
	SSM <sup>a</sup>	SD	SSM	SD	SSM	SD
15	0.962	$\pm 0.083$	0.253	$\pm 0.093$	0.955	$\pm 0.0766$
30	0.862	$\pm 0.046$	0.503	$\pm 0.092$	0.989	$\pm 0.06$
45	0.672	$\pm 0.048$	0.709	$\pm 0.087$	0.977	$\pm 0.06$
60	0.463	$\pm 0.046$	0.863	$\pm 0.09$	0.98	$\pm 0.059$
75	0.234	$\pm 0.079$	0.966	$\pm 0.088$	0.994	$\pm 0.073$

<sup>a</sup>SSM = sample statistical mean; SD = standard deviation.

Table 4 Normalized average restitution coefficients for 2024 aluminum target material at different incidence angles

Incidence angle $\beta_1$ , deg	Directional coefficient $e_\beta = \beta_2/\beta_1$		Velocity restitution coefficients				
			Tangential $e_T = V_{T2}/V_{T1}$		Normal $e_N = V_{N2}/V_{N1}$		Total $e_V = V_2/V_1$
	SSM <sup>a</sup>	SD	SSM	SD	SSM	SD	SSM
15	0.827	0.4	0.812	0.248	0.679	0.45	0.804
30	0.701	0.4	0.715	0.195	0.466	0.34	0.66
45	0.636	0.192	0.771	0.19	0.423	0.355	0.601
60	0.833	0.134	0.641	0.33	0.453	0.21	0.508
75	0.52	0.211	1.4	0.34	0.27	0.21	0.425

<sup>a</sup>SSM = sample statistical mean; SD = standard deviation.

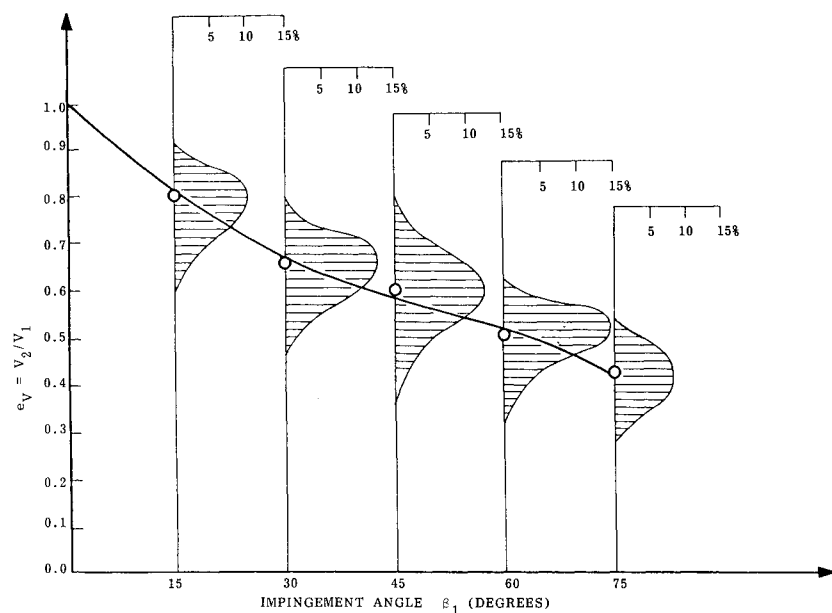


Fig. 5 Influence of impact angle on the particle velocity restitution coefficient.

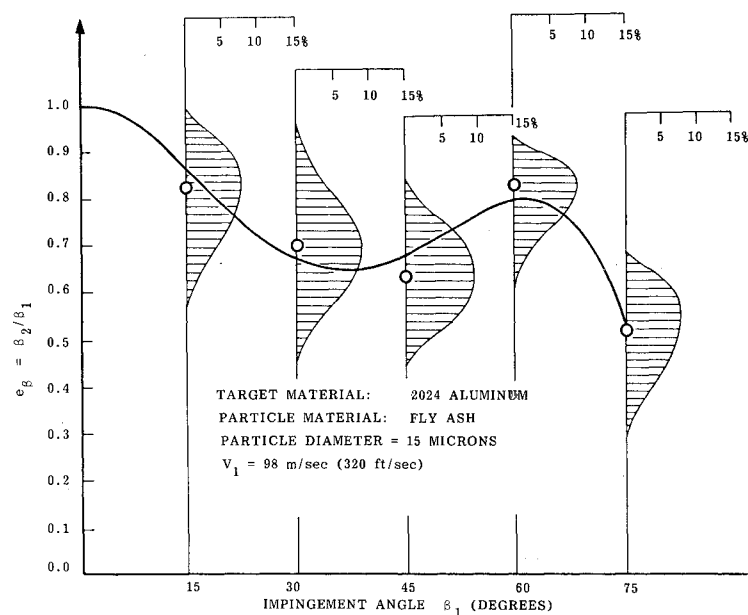


Fig. 6 Influence of impact angle on the particle directional coefficient.

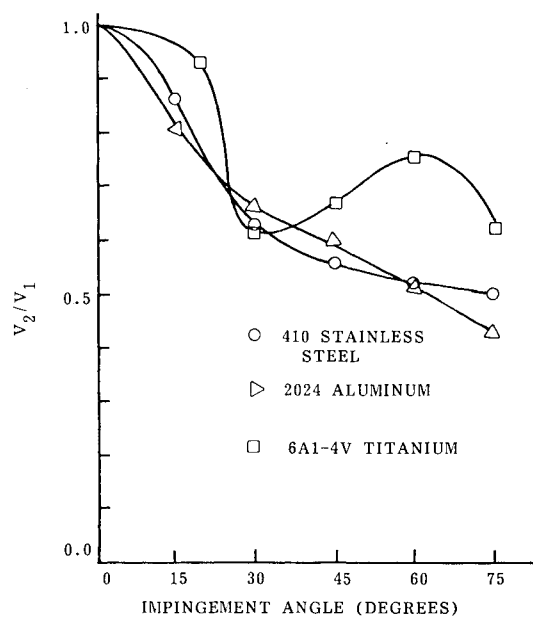


Fig. 7 Comparison of the particle velocity restitution ratio.

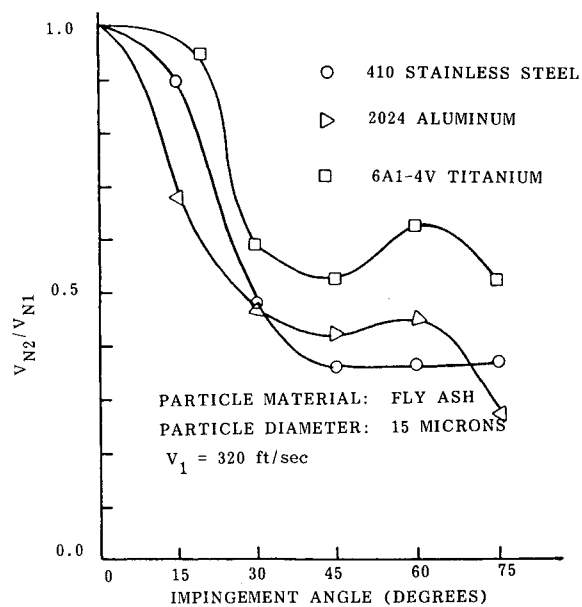
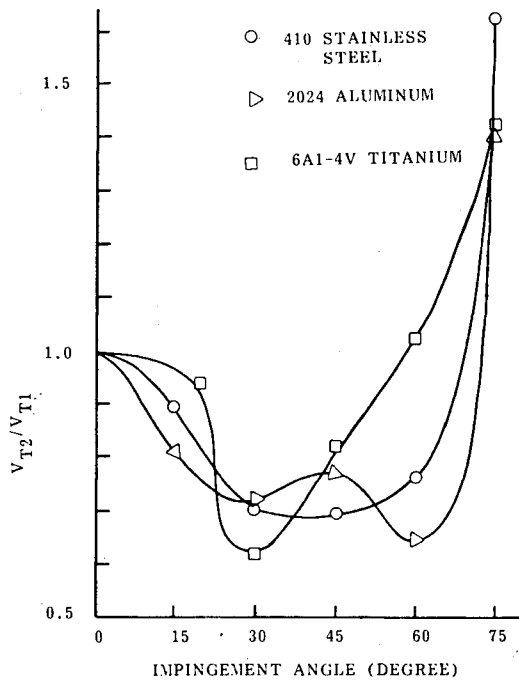


Fig. 8 Comparison of the particle normal velocity restitution ratio.

**Table 5** Normalized average restitution coefficients for 6A1-4V titanium target material at different incidence angles

Incidence angle $\beta_1$ , deg	Directional coefficient $e_\beta = \beta_2/\beta_1$		Velocity restitution coefficients				
			Tangential $e_T = V_{T2}/V_{T1}$		Normal $e_N = V_{N2}/V_{N1}$		Total $e_V = V_2/V_1$
	SSM <sup>a</sup>	SD	SSM	SD	SSM	SD	SSM
20	1.0	0.4	0.941	0.24	0.95	0.453	0.935
30	0.989	0.217	0.614	0.195	0.589	0.252	0.608
45	0.7	0.158	0.825	0.2	0.523	0.318	0.668
60	0.765	0.128	1.025	0.215	0.628	0.128	0.752
75	0.75	0.114	1.43	0.261	0.526	0.26	0.619

<sup>a</sup>SSM = sample statistical mean; SD = standard deviation.



**Fig. 9** Comparison of the particle tangential velocity restitution ratio.

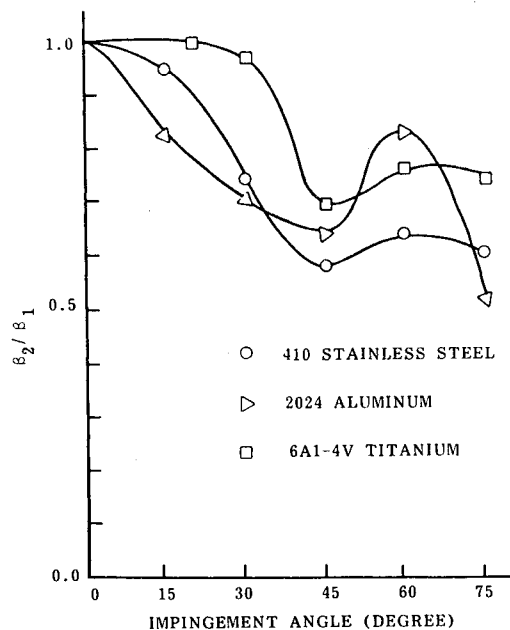


**Fig. 10** Comparison of the particle directional coefficient.

$$e_T = V_{T2}/V_{T1} = 1.07915 - 2.64204\beta_1 + 8.38479\beta_1^2 - 10.80932\beta_1^3 + 4.62071\beta_1^4 \quad (2)$$

$$e_N = V_{N2}/V_{N1} = 1.03047 - 1.08969\beta_1 - 1.40079\beta_1^2 + 3.65638\beta_1^3 - 1.75401\beta_1^4 \quad (3)$$

$$e_\beta = \beta_2/\beta_1 = 0.98877 + 0.29482\beta_1 - 4.83727\beta_1^2 + 7.65563\beta_1^3 - 3.3149\beta_1^4 \quad (4)$$

and for 6A1-4V titanium target material, they may be represented by the equations:

$$e_V = V_2/V_1 = 0.98965 + 0.96595\beta_1 - 6.83694\beta_1^2 + 9.30619\beta_1^3 - 3.68454\beta_1^4 \quad (5)$$

$$e_T = V_{T2}/V_{T1} = 1.01059 + 0.40772\beta_1 - 4.66001\beta_1^2 + 6.60803\beta_1^3 - 2.38436\beta_1^4 \quad (6)$$

$$e_N = V_{N2}/V_{N1} = 0.9709 + 1.52133\beta_1 - 8.56369\beta_1^2 + 10.5939\beta_1^3 - 3.93154\beta_1^4 \quad (7)$$

$$e_\beta = \beta_2/\beta_1 = 0.96605 + 0.87109\beta_1 - 3.13691\beta_1^2 + 2.74431\beta_1^3 - 0.71793\beta_1^4 \quad (8)$$

where  $\beta_1$  is measured in radians. All restitution coefficients are equal unity for  $\beta_1 = 0$ .

The above expressions may be used in the erosion equations developed by Grant and Tabakoff<sup>3</sup> to predict the erosion behavior of the materials. Similar measurements have been performed for 410 stainless steel as reported in Ref. 4. The obtained experimental data presented in Figs. 7–10 are important data for the particle trajectories calculation in turbomachinery or other industrial systems exposed to particulate flows.

### Conclusions

The dynamic impact characteristics of erosive fly ash particles impacting 2024 aluminum and 6A1-4V titanium materials with resulting rebound have been experimentally investigated. The results of this investigation have led to the following conclusions:

- 1) The kinetic energy lost by the particle can be expressed in terms of restitution coefficients. In theory, this parameter should then be proportional to the resulting erosion.
- 2) The restitution ratio decreases as the particle impact velocity increases.

3) Directional coefficients ( $\beta_2/\beta_1$ ) and restitution ratios for different alloys are different.

4) Particle restitution coefficients for particle sizes below 40  $\mu\text{m}$  can be measured only with LDV system.

5) The restitution parameters for fly ash particles over different target materials are measured for the first time and the data obtained can be of great benefit for trajectory calculations in turbomachinery or other systems exposed to such particles.

#### Uncertainty Analysis

A limited sample uncertainty analysis of Kline and McClintock<sup>5</sup> was used. The final velocities are found to have an uncertainty of 3%.

#### Acknowledgment

This research work was sponsored by U.S. Department of Energy Advanced Research and Technology Development Fossil Energy Material Program.

#### References

<sup>1</sup>Tabakoff, W. and Wakeman, T., "Test Facility for Material Erosion at High Temperature," ASTM SP 664, 1979, pp. 123-135.

<sup>2</sup>Kotwal, R. and Tabakoff, W., "A New Approach for Erosion Prediction due to Fly Ash," *Journal of Engineering for Power*, Vol. 103, April 1981, pp. 265-270.

<sup>3</sup>Grant, G. and Tabakoff, W., "Erosion Prediction in Turbomachinery Resulting from Environmental Solid Particles," *Journal of Aircraft*, Vol. 12, May 1975, pp. 471-478.

<sup>4</sup>Tabakoff, W. and Malak, M.F., "Laser Measurements of Fly Ash Rebound Parameters for Use in Trajectory Calculation," ASME Paper 85-GT-161, 1985.

<sup>5</sup>Kline, S.J. and McClintock, F.A., "Describing Uncertainties in Single-Sample Experiments," *Mechanical Engineering*, Vol. 75, Jan. 1953, p. 3.

## *From the AIAA Progress in Astronautics and Aeronautics Series . . .*

# **GASDYNAMICS OF DETONATIONS AND EXPLOSIONS—v. 75 and COMBUSTION IN REACTIVE SYSTEMS—v. 76**

*Edited by J. Ray Bowen, University of Wisconsin,  
N. Manson, Université de Poitiers,  
A. K. Oppenheim, University of California,  
and R. I. Soloukhin, BSSR Academy of Sciences*

The papers in Volumes 75 and 76 of this Series comprise, on a selective basis, the revised and edited manuscripts of the presentations made at the 7th International Colloquium on Gasdynamics of Explosions and Reactive Systems, held in Göttingen, Germany, in August 1979. In the general field of combustion and flames, the phenomena of explosions and detonations involve some of the most complex processes ever to challenge the combustion scientist or gasdynamicist, simply for the reason that *both* gasdynamics and chemical reaction kinetics occur in an interactive manner in a very short time.

It has been only in the past two decades or so that research in the field of explosion phenomena has made substantial progress, largely due to advances in fast-response solid-state instrumentation for diagnostic experimentation and high-capacity electronic digital computers for carrying out complex theoretical studies. As the pace of such explosion research quickened, it became evident to research scientists on a broad international scale that it would be desirable to hold a regular series of international conferences devoted specifically to this aspect of combustion science (which might equally be called a special aspect of fluid-mechanical science). As the series continued to develop over the years, the topics included such special phenomena as liquid- and solid-phase explosions, initiation and ignition, nonequilibrium processes, turbulence effects, propagation of explosive waves, the detailed gasdynamic structure of detonation waves, and so on. These topics, as well as others, are included in the present two volumes. Volume 75, *Gasdynamics of Detonations and Explosions*, covers wall and confinement effects, liquid- and solid-phase phenomena, and cellular structure of detonations; Volume 76, *Combustion in Reactive Systems*, covers nonequilibrium processes, ignition, turbulence, propagation phenomena, and detailed kinetic modeling. The two volumes are recommended to the attention not only of combustion scientists in general but also to those concerned with the evolving interdisciplinary field of reactive gasdynamics.

*Published in 1981, Volume 75—446 pp., 6×9, illus., \$35.00 Mem., \$55.00 List  
Volume 76—656 pp., 6×9, illus., \$35.00 Mem., \$55.00 List*

TO ORDER WRITE: Publications Dept., AIAA, 1633 Broadway, New York, N.Y. 10019